Available online at www.sciencedirect.com
SCIENCE DIRECT
International Journal of Non-Linear Mechanics 41 (2006) 304–312
INTERNATIONAL JOURNAL OF NON-LINEAR MECHANICS
www.elsevier.com/locate/nlm

Prediction of chaotic instabilities in a dragline bucket swing

Paul A. Meehan*, Kevin J. Austin

School of Engineering, University of Queensland, Brisbane, Qld. 4072, Australia

Received 28 January 2005; received in revised form 11 July 2005; accepted 8 August 2005

Abstract

The occurrence of chaotic instabilities is investigated in the swing motion of a dragline bucket during operation cycles. A dragline is a large, powerful, rotating multibody system utilised in the mining industry for removal of overburden. A simplified representative model of the dragline is developed in the form of a fundamental non-linear rotating multibody system with energy dissipation. An analytical predictive criterion for the onset of chaotic instability is then obtained in terms of critical system parameters using Melnikov's method. The model is shown to exhibit chaotic instability due to a harmonic slew torque for a range of amplitudes and frequencies. These chaotic instabilities could introduce irregularities into the motion of the dragline system, rendering the system difficult to control by the operator and/or would have undesirable effects on dragline productivity and fatigue lifetime. The sufficient analytical criterion for the onset of chaotic instability is shown to be a useful predictor of the phenomenon under steady and unsteady slewing conditions via comparisons with numerical results.

Keywords: Chaotic; Instability; Dragline; Melnikov's method; Multibody dynamics

1. Introduction

Multibody dynamical behaviour in a rotating multibody system is typically complex in nature, due to the non-linear interactions resulting from Coriolis and relative accelerations of components. Linear analyses of such systems are valid only within prescribed limits and approximations of the motion of component parts. Often a non-linear analysis is required to fully understand the dynamics and to enhance operation across a wide range of conditions. Recent attention has therefore concentrated on investigating non-linear instabilities, such as chaotic vibrations, that can arise in rotating multibody systems.

Moon [1] provides a wide review of physical systems that are known to exhibit chaotic vibrations, including a range of multibody systems. Mechanical systems of interest include helicopters, satellites, robotic manipulators and transmission mechanisms in trains and automobiles. Initial fundamental research includes contributions from Holmes and Marsden [2] and Koiller [3] on the non-linear behaviour of a rigid body with an attached flywheel. More recently, Meehan [4] has shown chaotic instability in a rotating body with a tuned mass damper [5], a torsional driveline incorporating a Hooke's Joint and a dual-spin spacecraft with dissipation. The primary contribution of the present research is the investigation of chaotic instabilities in another practical form of a fundamental rotating multibody system; namely a dragline.

Draglines are used as the primary means for removal of overburden in open-cut coal mining and are typically the bottleneck for productivity in this process. The dynamics of the dragline bucket swing motion during house slewing (rotation) is of particular importance from the viewpoint of structural loading and efficient operation [6]. Excessive amplitudes of this motion result in premature fatigue damage, undue wear of dragline components and could render the system difficult to control. Recent attempts at automation have focused on the dragline slewing phase of operation, however, an experienced human operator generally exceeds the performance of any artificial control system. This may be due to the inherently complex and non-linear regimes of dynamic conditions experienced by the dragline.

In this paper, a simplified formulation of the non-linear equations of motion governing the dynamics of the dragline system is presented. Global stability analysis results are then described and regions of non-linear behaviour are identified. Subsequently, the full analytical solution for the unperturbed system is obtained in order to identify homoclinic orbits. Once the

* Corresponding author. Tel.: +61 7 33 65 4320; fax: +61 7 33 65 4799.
E-mail address: meehan@uq.edu.au (P.A. Meehan).

0020-7462/$ - see front matter © 2005 Elsevier Ltd. All rights reserved.
doi:10.1016/j.ijnonlinmec.2005.08.004

system model is transformed into Hamiltonian form, Melnikov's method is applied to obtain an analytical criterion. Numerical and analytical results, describing the presence of chaotic instabilities under different operating conditions, are compared.

2. Modelling

A dragline system consists of a rotating assembly comprised of a house (containing primary components such as drive motors, controls and an operator cabin), a boom structure and a bucket, as shown in the simplified model of Fig. 1. The normal operation cycle consists of three main phases: (1) a digging phase, in which the bucket is filled with overburden; (2) a slew phase, in which the house and boom is swung (or slewed) about a vertical axis while the bucket is hoisted, and (3) a dump and return slew phase during which the overburden is dumped and the house and boom return to the dig position. Control of the hoist and drag rope lengths allows positioning of the bucket in the vertical boom plane. However, the bucket is free to swing normal to that plane and a considerable amount of operator skill is required to control this undesirable motion.

For the purposes of investigating non-linear behaviour associated with the predominant motions of the dragline, a simplified rotating multibody model based on Fig. 1 is developed. Referring to Fig. 1, the house and boom structure is modelled as a rigid body that rotates about the vertical axis with moment of inertia, I_h, and the bucket, a point mass that swings in the vertical plane with dissipation. The degrees-of-freedom of the system are given by θ and ϕ, describing the bucket swing rotation about A and rotation of the system about O, respectively. The bucket is centred on the body fixed y-axis at a distance h from A and has a point mass of m that moves in the yz-plane at a distance d from O. The bucket is considered to be acted upon by gravity, g, in the $-Y$ direction, and has a damping torque proportional to the bucket angular velocity. This damping torque is associated with viscous losses in the ropes and sheaves and has a constant, c_t. The instantaneous moment of inertia of the system about O, varies with the position of the bucket. For $\theta = 0$, the system is considered to have a moment of inertia I about the Y-axis. A net slew torque, M, about the Y-axis is generated from the slew transmission controlled by the operator.

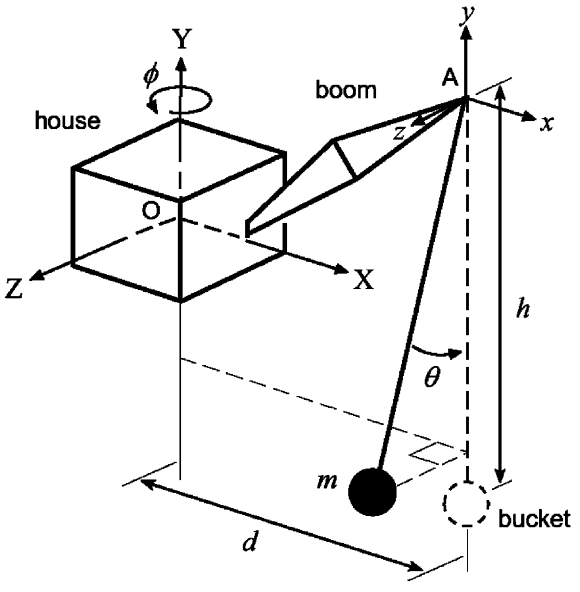

Fig. 1. Simple model of a slewing dragline.

The equations of motion for the system may be obtained using Lagrange's Equations with dissipation, as detailed in Appendix A. For convenience of stability analysis, these equations may be nondimensionalised to the form,

$$\left[\tilde{I} + \sin^2\theta\right]\phi'' + 2\phi'\theta'\sin\theta\cos\theta + \tilde{d}\left(\theta''\cos\theta - \theta'^2\sin\theta\right) = \tilde{M}, \tag{1}$$

$$\theta'' + 2\zeta\theta' + \left(1 - \phi'^2\cos\theta\right)\sin\theta + \tilde{d}\phi''\cos\theta = 0, \tag{2}$$

where the following dimensionless quantities are used:

$$\tau_\omega = \omega_o t, \quad \tilde{I} = \frac{I}{mh^2}, \quad \zeta = \frac{c_t}{2m\omega_o h^2}, \quad \tilde{d} = \frac{d}{h}, \quad \tilde{M} = \frac{M}{mh^2\omega_o^2} \tag{3}$$

and the natural frequency of the bucket swing under no slewing is $\omega_o = \sqrt{g/h}$. In (1) and (2), the prime notation $()'$ denotes differentiation with respect to dimensionless time, τ_ω. Eq. (1) can be considered to be the moment equation in the XZ plane. The coefficient of ϕ'' in Eq. (1) represents the instantaneous moment of inertia of the system about O, while the last two terms represent the moments arising from the Coriolis and other inertia forces with respect to O. Eq. (2) represents the moment equation for the bucket motion in the boom fixed yz plane. The first three terms are typical for a damped pendulum, while the last two terms characterise the effects of the centrifugal and angular accelerations, arising due to the moving reference plane. Eqs. (1) and (2) are coupled through three non-linear terms resulting from the rotating multibody motion of the system.

For subsequent analysis, it is convenient to define the energy and angular momentum quantities that are conserved under unperturbed conditions. The derivations of these quantities are found in Appendix A. The total mechanical energy of the system, E, may be derived in nondimensional form as

$$\tilde{E} = \tfrac{1}{2}\left(\tilde{I} + \sin^2\theta\right)\phi'^2 + \tfrac{1}{2}\theta'^2 + \tilde{d}\phi'\theta'\cos\theta + 1 - \cos\theta, \quad \text{where } \tilde{E} = \frac{E}{mh^2\omega_o^2}. \tag{4}$$

Similarly, the y component of angular momentum of the system about O, H_{Oy}, that is conserved when $M = 0$, may also be

obtained as

$$\tilde{H}_{Oy} = \left(\tilde{I} + \sin^2\theta\right)\phi' + \tilde{d}\theta'\cos\theta,$$
$$\text{where } \tilde{H}_{Oy} = \frac{H_{Oy}}{mh^2\omega_o}. \tag{5}$$

For the subsequent analysis, the magnitude of the bucket swing angle, θ, is considered to be small $(\lesssim \pi/10$ *radians*$)$, in line with realistic operation of the dragline system.

3. Stability analysis

The stability analysis of the system was facilitated by reducing the order of the system by one using the constant angular momentum as a system parameter. As such, for the following stability analysis, the case of no external torque, $M = 0$, is considered so that the total angular momentum of the system, H_{Oy}, is equal to a constant. The critical points for the homogenous system may then be found by setting $[\theta' \ \theta'' \ \phi''] = [0\ 0\ 0]$ and using Eqs. (1), (2) and (5) to obtain three equilibrium points

$$[\theta \quad \phi']^{\mathrm{T}} = [0 \quad \phi'^*]^{\mathrm{T}},$$
$$\left[\pm\theta^* \quad 1/\sqrt{\cos\theta^*}\right]^{\mathrm{T}} \quad \text{if } \tilde{H}_{Oy} > \tilde{I},$$
$$\left[\pm\theta^* \quad -1/\sqrt{\cos\theta^*}\right]^{\mathrm{T}} \quad \text{if } \tilde{H}_{Oy} < -\tilde{I}, \tag{6}$$

where $\phi'^* = \tilde{H}_{Oy}/\tilde{I}$ and θ^* is a function of the parameters, $\tilde{H}_{Oy}$ and $\tilde{I}$, as defined by the roots of a fourth order polynomial

$$\theta^* = \cos^{-1}\left[\text{root}\left(\left(\tilde{I} + 1 - x^2\right)^2 - \tilde{H}_{Oy}^2 x = 0\right)\right]. \tag{7}$$

By inspection of Eqs. (6) and (7), it may be deduced that the equilibrium configuration depends on the angular momentum of the system and that the magnitude of θ^* is always less than $\pi/2$.

The stability of the equilibrium points was investigated using Lyapunov's direct method, as detailed in Appendix B. This stability analysis revealed that the first equilibrium point described by $[\theta\ \phi']^{\mathrm{T}} = \left[0\ \hat{H}_{Oy}/\hat{I}\right]^{\mathrm{T}}$, is globally asymptotically stable if

$$\tilde{H}_{Oy}^2 \leqslant \tilde{I}^2 \quad \text{and} \quad \tilde{I} > \tilde{d}^2. \tag{8}$$

The other equilibrium points, described by $\left[\theta^2\ \phi'^2\right]^{\mathrm{T}} = \left[\theta^{*2}\ 1/\cos\theta^*\right]$, are globally asymptotically stable if

$$\tilde{H}_{Oy}^2 > \tilde{I}^2 \quad \text{and} \quad \tilde{I} > \tilde{d}^2. \tag{9}$$

The condition $\hat{I} > \hat{d}^2$ is always satisfied by real system parameters since the system inertia, I, must be greater than the point mass inertia contribution, md^2.

From this analysis the sign of the equilibrium slew velocity, ϕ'^*, for the first of these equilibrium points is found to be directly dependent on the sign of the initial angular momentum of the system. It is also noticed that under no external torque ($M = 0$), the system is dissipative and the steady state behaviour of the system can be predicted precisely using Eqs. (4)–(9) and qualitatively by noting the angular momentum is conserved but the final energy is minimised. As an example, for initial conditions such that the angular momentum is described by $H_{Oy}^2 > I^2\omega_o^2$, the first stability condition described by Eq. (8) is violated, so that either one of the latter two equilibrium points described by Eq. (6) become the dominant attractor, depending on the sign (or direction) of the angular momentum of the system, H_{Oy}. The symmetrical properties of the bucket swing allow the possibility of motion about two stable equilibrium points, corresponding to positive and negative rotational displacements of the bucket mass, $\pm\theta^*$. In order to investigate this property further, a phase space analysis was performed.

4. Phase space analysis

The phase space of the unperturbed system, corresponding to the case of no external torque $\tilde{M} = 0$ and no damping $\tilde{f} = 0$, was investigated for non-linear behaviour. For the unperturbed system, both angular momentum and total energy of the system have constant values $\tilde{H}_{Oy}$ and $\tilde{E}$, such that by using Eqs. (4) and (5), the phase space may be described by

$$\theta'^2 = \frac{2\left(\tilde{I} + \sin^2\theta\right)\left(\tilde{E} - 1 + \cos\theta\right) - \tilde{H}_{Oy}^2}{\tilde{I} - \tilde{d} + \left(1 + \tilde{d}\right)\sin^2\theta}. \tag{10}$$

This equation may be shown to be integrable; a necessary condition for application of Melnikov's method. The corresponding set of phase curves for different values of $\tilde{E}$ are plotted in Fig. 2. These phase space plots are representative of the unperturbed dynamics of the dragline system for out of plane bucket angles of magnitude less than π.[1] Fig. 2a corresponds to the last two equilibrium conditions described by Eq. (6), while Fig. 2b corresponds to the first. The existence of a pair of homoclinic orbits in Fig. 2a encircling the two equilibrium points is important to note. The system will be attracted to either one of the equilibrium points depending on the initial conditions and there will be a region in phase space where this dependence will be highly sensitive to small changes. By solving for the origin point using Eq. (10), the set of homoclinic orbits is found to occur under the condition

$$\tilde{C} = 2\tilde{E}\tilde{I} - \tilde{H}_{Oy}^2 = 0. \tag{11}$$

The homoclinic orbits described in Fig. 2 will be considered for the application of Melnikov's method. It may be deduced that

[1] For larger, unrealistic, out of plane bucket angles, the phase space has heteroclinic orbits intersecting at the unstable equilibrium points defined by $\theta = \pm n\pi$, similar to the phase space of a simple pendulum.

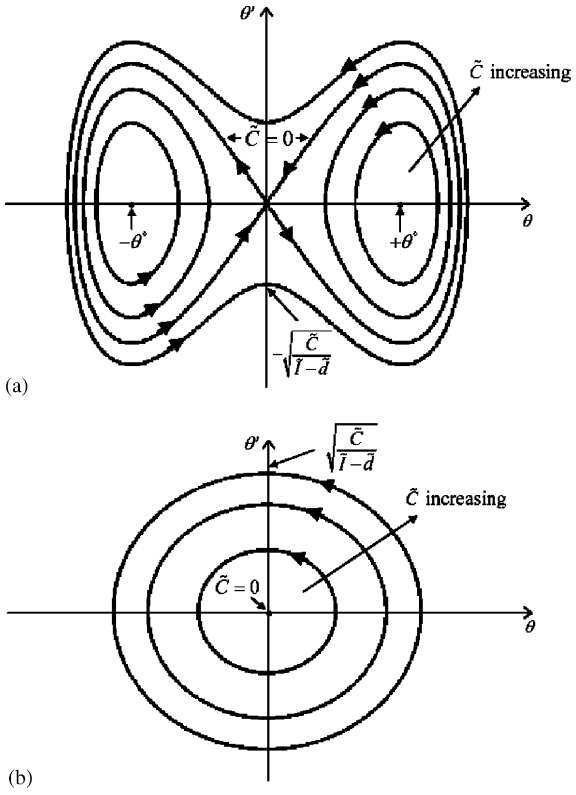

Fig. 2. Phase space curves for slewing dragline model, (a) $\hat{H}_{oy}^2 > \hat{I}^2$; (b) $\hat{H}_{oy}^2 \leqslant \hat{I}^2$.

the homoclinic orbits in Fig. 2a first exist and are smallest when the angular momentum first exceeds the critical value described by Eq. (9). Therefore it is expected that any onset of chaotic instability will first occur for small bucket swing angles.

5. Melnikov's method

Melnikov's method was used to obtain an analytical criterion for the onset of chaotic instability in the perturbed dragline system based upon the unperturbed phase space. The simplest form of Melnikov's method considers systems of the form:

$$\dot{\mathbf{x}} = \mathbf{f}(\mathbf{x}) + \varepsilon \mathbf{g}(\mathbf{x}, t); \quad \mathbf{x} = \begin{pmatrix} u \\ v \end{pmatrix} \in \Re^2, \tag{12}$$

where $\mathbf{f}(\mathbf{x})$ is considered to be the unperturbed Hamiltonian system of state equations defined on $\Re^2$, and $\varepsilon \mathbf{g}(\mathbf{x}, t)$ is a small periodic perturbation which is not necessarily Hamiltonian. In order to apply Melnikov's method on the dragline system, the equations of motion (1) and (2) need to be transformed to the form of (12). Under the assumption of a small bucket swing angle, the harmonic terms of (1) and (2) are approximated by

$$\sin\theta \approx \theta, \quad \cos\theta \approx 1 \tag{13}$$

and the system equations of motion reduce to a form similar to that of a rotating body with internal energy dissipation [5]. Therefore, it is convenient to transform the dragline model into this form using the dimensionless quantities,

$$\tau_\Omega = \Omega t, \quad \hat{y} = \frac{\theta}{\tilde{d}}, \quad \tilde{\Omega} = \frac{\Omega}{\omega_o}, \quad \hat{I} = \frac{\tilde{I}}{\tilde{d}^2}, \quad \hat{c} = \frac{2\zeta}{\tilde{\Omega}},$$
$$\hat{k} = \frac{1}{\tilde{\Omega}^2}, \quad \hat{M} = \frac{\tilde{M}}{\tilde{d}^2\tilde{\Omega}^2}, \quad \hat{H}_{Oy} = \frac{\tilde{H}_{Oy}}{\tilde{d}^2\tilde{\Omega}}, \tag{14}$$

where Ω is the frequency of the perturbing torque. Using (13) and (14), the equations of motion (1) and (2) can be expressed in Hamiltonian form as

$$\mathrm{d}\hat{y}/\mathrm{d}\tau_\Omega = \hat{p}_y \left(\hat{I} + \hat{y}^2\right)\left(\hat{I} - 1 + \hat{y}^2\right)^{-1},$$

$$\begin{aligned}\mathrm{d}\hat{p}_y/\mathrm{d}\tau_\Omega = {} & \frac{\hat{y}}{(\hat{I}+\hat{y}^2)^2} \\ & \times \left\{\hat{H}_{Oy}^2 - \hat{k}\left(\hat{I}+\hat{y}^2\right)^2 + \left[\hat{p}_y\left(\hat{I}+\hat{y}^2\right)\beta(\hat{y})\right]^2\right\} \\ & + \varepsilon\left[\hat{M}_\mathrm{E}\cos\tau + 2\hat{y}\hat{M}_\mathrm{E}\left(\hat{H}_{Oy}/\hat{I}\right)\sin\tau\right. \\ & \left. + \hat{y}\left(\hat{M}_\mathrm{E}^2/\hat{I}\right)\sin^2\tau - \hat{c}\hat{p}_y\left(\hat{I}+\hat{y}^2\right)^2\beta(\hat{y})\right] \\ & + O\left(\varepsilon^2\right),\end{aligned} \tag{15}$$

where the generalised momentum, $\hat{p}_y$, is defined by

$$\hat{p}_y = \hat{y}'\left(\hat{I} - 1 + \hat{y}^2\right)/\left(\hat{I}+\hat{y}^2\right) \tag{16}$$

and a slew torque of the form $\hat{M} = \hat{M}_\mathrm{E}\cos\tau$ is considered. For Eq. (15), a Taylor's series has been used to expand the perturbational terms with $\varepsilon = 1/\hat{I}$, so that only first order terms have been retained. More details of this transformation are provided in Meehan [4]. It is noted that the unperturbed phase space $\{\hat{y}, \hat{p}_y\}$, will have the same qualitative behaviour as the phase space $\{\theta, \theta'\}$, illustrated in Fig. 2.

Eq. (15) is in the form appropriate for the application of Melnikov's method. For brevity, the primary steps of the Melnikov analysis are outlined, as details of a very similar analysis is provided in Meehan [4]. The Melnikov function, denoted $\mathscr{M}(t_0)$ is written as the integral

$$\mathscr{M}(t_0) = \int_{-\infty}^{\infty} \mathbf{f}(\mathbf{q}_0(t)) \wedge \mathbf{g}(\mathbf{q}_0(t), t + t_0)\, \mathrm{d}t, \tag{17}$$

where $\mathbf{f}(\mathbf{x})$ and $\mathbf{g}(\mathbf{x}, t)$ have been defined previously in Eq. (12), the symbol $\wedge$ is the wedge product defined by $a \wedge b = a_1 b_2 - a_2 b_1$, and $\mathbf{q}_0(t)$ is the solution for the set of homoclinic orbits in the unperturbed system. The equations describing the homoclinic orbits depicted in Fig. 2a, for small out of plane angle, θ, may be obtained via solution to Eqs. (10), subject to (11), (13) and (14), as

$$\begin{aligned}\left[\hat{y}_0 \quad \mathrm{d}\hat{y}_0/\mathrm{d}\tau_\Omega\right] = {} & \left[\sqrt{\eta}\,\mathrm{sech}(\vartheta\tau_\Omega)\right. \\ & \left. -\vartheta\sqrt{\eta}\,\mathrm{sech}\,(\vartheta\tau_\Omega)\tanh(\vartheta\tau_\Omega)\right],\end{aligned} \tag{18}$$

where

$$\eta = \left(2\tilde{E} - \tilde{I}\right)/\tilde{d}^2, \quad \vartheta = \sqrt{\left(2\tilde{E} - \tilde{I}\right)/\left(\tilde{I} - \tilde{d}^2\right)}/\Omega \tag{19}$$

and the subscript $()_0$ denotes the closed solution for the homoclinic orbits. Using Eqs. (18), (12) and (15) the Melnikov function may be obtained explicitly. In particular, under the assumption that $\hat{M}_E \ll \hat{I}\sqrt{\hat{k}/\left(\hat{I}-1\right)}$ or $\hat{M}_E \ll 2\hat{H}_{Oy}\cosh(\pi/2\vartheta)$, a relationship for the critical torque amplitude may be expressed as

$$\hat{M}_E > 2\hat{c}\vartheta^3\left(5\hat{I}+2\eta\right)\Bigg/\left(15\pi\sqrt{\frac{\vartheta^2}{\eta}\operatorname{sech}^2\left(\frac{\pi}{2\vartheta}\right)+\frac{\hat{H}_{Oy}^2}{\hat{I}^2}\operatorname{cosech}^2\left(\frac{\pi}{2\vartheta}\right)}\right). \qquad (20)$$

Eq. (20) represents a sufficient criterion for the occurrence of chaotic instability in a dragline under slew torque perturbations, for small bucket swing angles. It is based on perturbations about a nominal (unperturbed) condition of constant (or quasistatic) angular momentum. In the context of a dragline, this unperturbed condition represents a constant slewing of the dragline in one direction, known as "dumping on the fly", when slew angles close to 180° are required. The criterion may also be considered to be based upon instantaneous quasistatic conditions during the swing or return swing phases of normal operation. In the following analysis, the occurrence of chaotic instabilities under these steady slewing conditions is investigated before extending the analysis to represent normal (unsteady) slewing operation.

6. Chaotic instability in a dragline under steady slewing

Predictions of the occurrence of chaotic instability in a dragline under steady slewing motion were investigated both analytically and numerically for realistic dragline parameters. For this study, the mechanical parameters for a standard 1370 BE dragline were used: m=66 000 kg, c_t=4.1 MNms, d=87 m, $h=100$ m, $I_h = 1.588\times10^9$ kg m^2 and $\Omega = 0.05 \rightarrow 0.2$ rad/s. For these parameters, the natural frequency of the bucket swing under no slew conditions is, $\omega_0 = 0.31321$ rad/s. Slew conditions were chosen to represent typical operational conditions. In particular, the slew torque frequency was chosen to be of the same order as the actual swing cycle used in dragline operation. According to the criterion of Eq. (20), initial slew rates approaching the critical value of ω_o (from above) were investigated to minimise the critical torque amplitude to values within the maximum slew torque available on current draglines (of order 50 MNm). Numerical integration of Eqs. (1) and (2) was performed using a Huen predictor–corrector method with at least 80 timesteps over the bucket response cycle; ensuring convergence of the numerical solution. Plots were generated after a number of pre-iterates (no recording) of forcing periods, in order to ensure transients had subsided.

Fig. 3 shows an example of a bifurcation diagram generated for an initial slew rate of $\dot{\phi}_i = 0.32$ rad/s, a slew torque frequency of 0.05 rad/s and 200 pre-iterates. The diagram shows evidence of chaotic instability for increasing torque amplitudes characterised by period doubling bifurcations. The initial occurrence of steady state chaotic instability may be seen to occur with a disturbance slew torque amplitude of approximately $M_E = 390$ kNm. In the same manner, the critical torque amplitudes for a number of bifurcation diagrams at different slew torque frequencies were determined in order to obtain a quantitative comparison with analytical predictions using Eq. (20). Fig. 4 summarises these results and highlights the conservative nature of the Melnikov criterion for predicting the onset of steady-state chaotic instability. The agreement between the analytical and numerical results is typical of similar

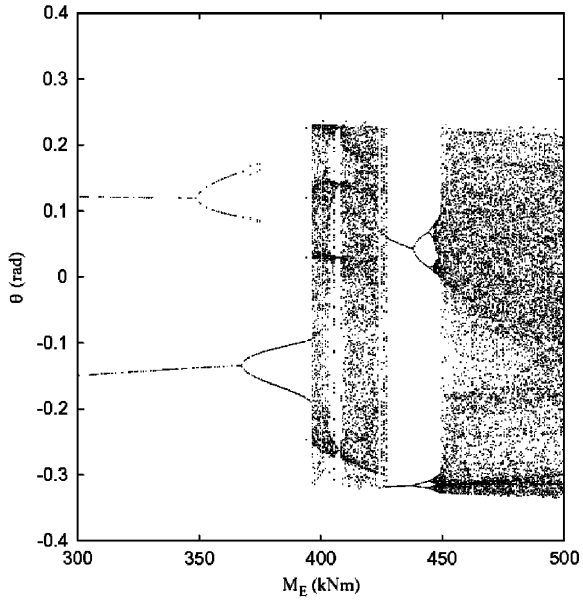

Fig. 3. Bifurcation diagram for the dragline under steady slew (ϕ) conditions.

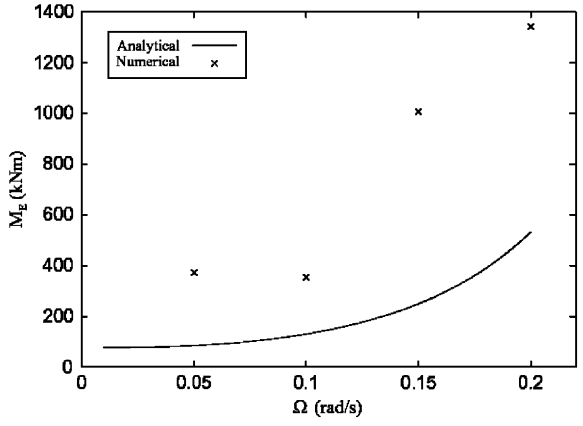

Fig. 4. Comparison of analytical and numerical results for the chaotic instability of the dragline bucket swing under steady slew conditions.

investigations using Melnikov's method,[2] such as Meehan [4], Miller et al. [7] and Moon [1].[3] These results, under steady slewing conditions, also indicate that the dragline motion may pass through chaotic instability during a normal (unsteady slewing) cycle of operation.

7. Chaotic instability in a dragline under unsteady slewing

With the onset of chaotic instability evident under steady slewing conditions, it was reasonable to investigate the occurrence of chaotic instability during the unsteady slewing conditions characteristic of normal dragline operation. For this case, an unsteady slew torque from stationary initial conditions (at dig) is considered of the form,

$$\hat{M} = \hat{M}_{\mathrm{Eu}} \cos(\tau_\Omega) - \hat{c}_{\mathrm{h}}(\mathrm{d}\phi/\mathrm{d}\tau_\Omega), \quad \text{where } \hat{c}_{\mathrm{h}} = c_{\mathrm{h}}/(I\Omega) \tag{21}$$

and c_{h} is the house slew damping constant that arises due to rotational dissipation and/or derivative motor control. In order to use criterion (20) in this case, an equivalent unperturbed angular momentum, $\hat{H}_{Oy}$, and slew torque amplitude $\hat{M}_{\mathrm{E}}$, need to be determined. The equivalent quantities may be considered to be the quasistatic maxima of these parameters under unsteady slewing conditions. In particular, by assuming small bucket swing angles, such that the effect of this motion on the maximum angular momentum is small, Eqs. (1), (5), (14) and (21) may be solved to give an approximate maximum torque amplitude and angular momentum of

$$\hat{H}_{Oy_{\max}} = \hat{M}_{\mathrm{E}_{\max}} = \hat{M}_{\mathrm{Eu}} \Big/ \sqrt{1+\hat{c}_{\mathrm{h}}^2}. \tag{22}$$

The critical torque amplitude under unsteady slewing conditions can then be obtained by substituting (22) into (20) and solving for $\hat{M}_{\mathrm{Eu}}$. Under unsteady conditions it is important to realize that this resultant criterion for chaotic instability is only applicable when the homoclinic orbits of Fig. 2a exist. Based on Eqs. (9) and (22) the condition for the existence of homoclinic orbits under unsteady slewing conditions may be expressed as the nondimensional or dimensional inequality,

$$\hat{M}_{\mathrm{Eu}} > \hat{I}\hat{k}\sqrt{1+\hat{c}_{\mathrm{h}}^2} \quad \text{or}$$

$$M_{\mathrm{Eu}} > I\omega_{\mathrm{o}}\Omega\sqrt{1+(c_{\mathrm{h}}/(I\Omega))^2}. \tag{23}$$

Therefore, the criterion for the onset of chaotic instability is defined by both the conditions of Eqs. (20) and (22), as well as (23).

The accuracy of this analytical criterion was investigated via numerical simulations of typical unsteady slewing conditions, with a nominal slew torque frequency of $\Omega = 0.0623$ rad/s representing a cycle time of 100 s. All other parameters were set values as specified previously, with exception to house slew damping, which was set to a value of $c_{\mathrm{h}} = 8.97 \times 10^7$ Nm s;

[2] Melnikov's method provides a sufficient criterion for transient chaos, whereas the bifurcation diagrams indicate the onset of steady state chaotic instability.

[3] pp. 267–268.

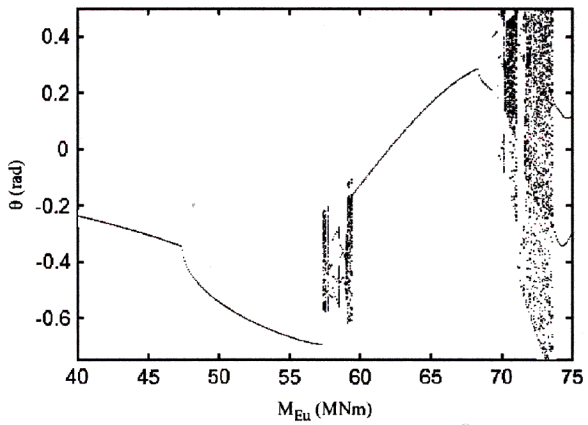

Fig. 5. Bifurcation diagram for the dragline under unsteady slew (ϕ) conditions.

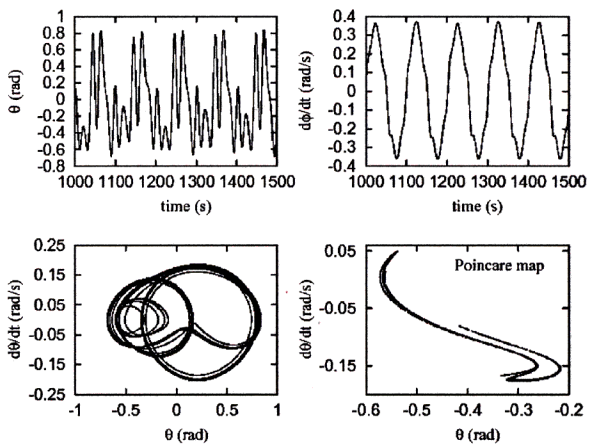

Fig. 6. Chaotic bucket response for a dragline under normal (unsteady) slewing conditions, where $M = 57 \times 10^5$ Nm.

obtained from field measurements. The bifurcation diagram of Fig. 5 was generated under these conditions and indicates the first onset of chaotic instability at a torque amplitude of approximately 57 MNm. This value compares favourably with the analytical prediction of 49.5 MNm from (20) and (22). Trajectory simulations and the Poincare map for this torque amplitude are shown in Fig. 6. The complexity of the time history and phase space traces and the fractal nature of the Poincare map are consistent with predictions of chaotic instability. These numerical simulations confirm that chaotic behaviour could occur, even though the house only has the necessary slew rate for homoclinic orbits to exist, for a relatively small amount of cycle time.

In Fig. 7, numerical results were plotted in the same manner as described for Fig. 4, along with the analytical solution to Eqs. (20) and (22) as well as the approximate criterion of (23). The circled cases indicate results with bucket swing angle amplitudes greater than one complete revolution. The two analytical solutions were found to overlap, confirming that the approximate criterion (23) dominates for the unsteady dragline conditions. By inspection of the analytical and numerical results, it is seen that the approximate criterion (23) provides

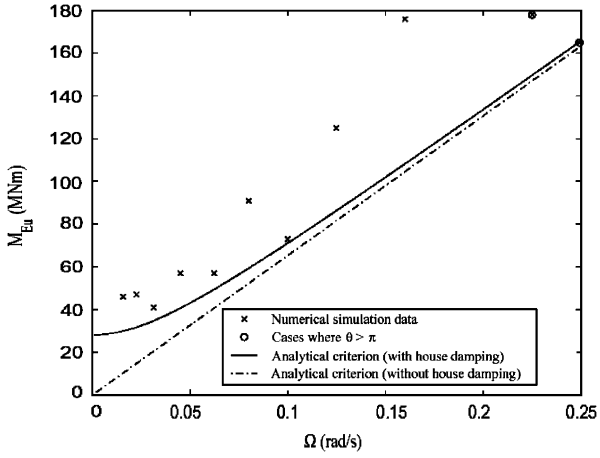

Fig. 7. Comparison of analytical and numerical results for the chaotic instability of the dragline bucket swing under unsteady slew conditions.

Table 1
Critical slew torque amplitude sensitivity to process parameters

Parameter description		Change in critical torque amplitude* (%)
House inertia	(I_h)	+5.1
Bucket mass	(m)	+1.6
Hoist rope length	(h)	−4.7
Horizontal distance of bucket from slew axis	(d)	+3.3
Bucket swing damping	(c_t)	≈ 0
House slew damping	(c_h)	6.7
Slew torque frequency	(Ω)	10.5

*Due to a +10% change in parameter based on nominal dragline conditions.

a useful conservative prediction for the onset of chaotic instability over a wide range of slew torque frequencies. Fig. 7 also shows a plot of the critical slew torque for the case of no house slew damping. The stabilising effect of house slew damping is seen to be greater for lower torque frequencies, in line with (23).

Based on these results it was of interest to investigate the effect of changes in dragline parameters on the critical slew torque amplitude. Using Eqs. (20)–(23), the percentage changes in critical torque amplitude due to a 10% increase in the dragline parameters were determined and are presented in Table 1. It is noted that results of similar magnitude but of opposite sign were obtained for a 10% decrease. The sensitivity results are in accordance with the predictions of the approximate criterion (23) on it's own, confirming the previous results. This indicates that the lower bound for critical torque amplitude is determined solely by the natural frequency (rope length), the system inertia (house inertia, bucket mass and position), house slew damping and the period for a cycle. In particular, for a given slew angle range (governed by the dig and dump points), the system is most sensitive to changes in house inertia, slew damping and the hoist rope length. House inertia provides the main contribution to the system inertia (76%), hence the effect of changes in bucket mass is less as it only contributes approximately 24%. The critical torque amplitude is twice as sensitive to changes in the bucket horizontal position, d, as compared to mass, m, due to the md^2 contribution to the system inertia. It may be inferred that the onset of chaotic instability is relatively insensitive to dragline boom size since the effects of changes in d and h tend to cancel each other. In general, the predictions of Table 1 were found to be evident in numerical simulations using bifurcation diagrams.

8. Conclusion

Analytical and numerical results have shown the existence of chaotic instabilities in a model of a dragline with internal energy dissipation, under perturbed steady slewing as well as normal unsteady conditions. In particular, closed form analytical criteria and numerical verification of these predictions of chaotic instability are presented in this fundamental rotating multibody system. An analytical criterion for the occurrence of a chaotic instability region in system parameter space has been derived using Melnikov's analysis. The chaotic region occurs near homoclinic orbits in the system's phase space, which may exist in the dynamics of a slewing dragline with damping under normal operation. Subsequently the analytical results have been compared to various numerical results for different parameter configurations. It is shown that Melnikov's method provides a conservative estimate for the onset of steady state chaotic instability. In particular, the results confirm that the analytical criteria are useful for predicting and avoiding the onset of chaotic instability in a dragline under steady and unsteady slewing conditions. Chaotic instability is shown to occur more readily for a higher slew torque amplitude, lower slew torque frequency, lower house inertia and for slew rates close to but greater than the natural frequency of the bucket pendulum-like motion.

From this analysis it would appear that steady state chaotic instability is possible in dragline operating cycles, during high slew rate conditions. Its occurrence adversely affects dragline productivity and maintenance, and may be underlying difficulties with automation. With present trends in technology towards increasing power and decreasing dragline inertia, it is expected that this phenomenon may become more prevalent. The present analysis provides identification of the critical parameters associated with the phenomenon and a design tool by which to avoid its occurrence. Recommendations for useful extensions to the analysis include the investigations of; a more realistic slew torque profile, the effects of digging/bucket load force changes, a range of bucket positions, changing constraints and catenary effects of the dragline ropes during normal cycle operation.

Acknowledgements

The authors acknowledge the support of the UQ Early Career Research Grant Scheme and Mr Sern Jee for his assistance in compiling the paper.

Appendix A. Derivation of equations of motion

The equations of motion of the dragline model described in Fig. 1 may be derived using Lagrange's Method in a similar manner to that described in Corke et al. [6]. In particular, the kinetic energy of the system, T, may be considered to be the sum of components arising from the motion of the inertia of the house and boom, I_h, and that of the bucket mass, respectively, such that,

$$T = \tfrac{1}{2} I_h \dot{\phi}^2 + \tfrac{1}{2} m \dot{\mathbf{r}}^2, \tag{A.1}$$

where $\dot{\mathbf{r}}$ is the velocity vector of the bucket point mass in the inertial frame of reference O. By use of elementary coordinate frame transformations from the frame of reference A, the position vector of the bucket point mass, $\mathbf{r}$, may be determined in the inertial frame of reference O as

$$\mathbf{r} = (d\cos\phi - h\sin\theta\sin\phi)\hat{\mathbf{i}} - h\cos\theta\hat{\mathbf{j}} - (d\sin\phi + h\sin\theta\cos\phi)\hat{\mathbf{k}}, \tag{A.2}$$

where $\hat{\mathbf{i}}$, $\hat{\mathbf{j}}$, $\hat{\mathbf{k}}$ are the unit vectors along the X, Y, Z axes, respectively.

The potential energy due to gravity is proportional to the bucket vertical position and may be defined as

$$V = mgh(1 - \cos\theta), \tag{A.3}$$

where potential energy is defined as being zero when the bucket swing angle $\theta = 0$. The energy dissipated due to bucket swing motion may be defined as

$$D = \tfrac{1}{2} c_t \dot{\theta}^2. \tag{A.4}$$

Substitution of expressions for T, V and D from Eqs. (A.1–A.4) into Lagranges equation yields the equation of motion for the generalised parameters $q_1 = \phi$ and $Q_1 = M$ as

$$\left[I + m(h\sin\theta)^2\right]\ddot{\phi} + 2m(h\sin\theta)\frac{\mathrm{d}}{\mathrm{d}t}(h\sin\theta)\dot{\phi} + md\frac{\mathrm{d}^2}{\mathrm{d}t^2}(h\sin\theta) = M, \tag{A.5}$$

where

$$I = I_h + md^2. \tag{A.6}$$

Similarly, the equation of motion for the torque balance associated with the bucket swing motion may be derived for $q_2 = \theta$ and $Q_2 = 0$ as

$$mh^2\ddot{\theta} + c_t\dot{\theta} + mgh\sin\theta - mh^2\sin\theta\cos\theta\dot{\phi}^2 + mdh\cos\theta\ddot{\phi} = 0, \tag{A.7}$$

where the last two terms characterise the effects of the centrifugal and angular accelerations respectively. Eqs. (A.5) and (A.7) completely describe the system dynamics, which is of order five since M is assumed to vary periodically with time.

For the purposes of stability analysis it is convenient to define the energy and angular momentum quantities that are conserved in unperturbed conditions. The total mechanical energy of the system, E, is simply given by $T + V$ using Eqs. (A.1–A.3). The y component of angular momentum of the system about O, that is conserved when $M = 0$, may also be expressed as

$$H_{Oy} = I_h\dot{\phi} + \mathrm{comp}_{\hat{\mathbf{j}}}(m\mathbf{r}\times\dot{\mathbf{r}}) = \left(I + m(h\sin\theta)^2\right)\dot{\phi} + md\frac{\mathrm{d}}{\mathrm{d}t}(h\sin\theta). \tag{A.8}$$

Appendix B. Stability of equilibrium points using Lyapunov's direct method

For each of the critical points $\mathbf{X}_{eq}$ described by Eq. (6), a suitable Lyapunov function for the system may be chosen using the total mechanical energy of the system in the form $\tilde{L} = \tilde{E} - \tilde{E}_C$, where $\hat{E}_C$ is a constant equal to the total energy at a particular critical point. This may be expressed in terms of $\mathbf{X} = [X_1\ \ X_2\ \ X_3]^T = [\theta\ \ \theta'\ \ \phi]^T$ using Eqs. (4) and (5) as

$$\tilde{L} = \left[\tilde{H}_{Oy}^2 - \left(\tilde{d}X_2\cos X_1\right)^2\right] / \left[2\left(\tilde{I} + \sin^2 X_1\right)\right] + X_2^2/2 + 1 - \cos X_1 - \hat{E}_C. \tag{B.1}$$

By the use of Eqs. (1) and (2), the time derivative of this function may be obtained as

$$\tilde{L}' = \tilde{E}' = -2\zeta X_2^2 + \tilde{M}X_3. \tag{B.2}$$

Under the condition of no external torque, $\tilde{M} = 0$, inspection of (B.2) reveals that $\tilde{L}'$ is negative semi-definite. It may also be noted that $\tilde{L}(\mathbf{X}) \to \infty$ as $\|\mathbf{X}\| \to \infty$, indicating that the Lyapunov function $\tilde{L}$ is radially unbounded. Under these conditions, asymptotic stability cannot usually be concluded since $\tilde{L}'$ is negative semi-definite. However, by the use of the theorem described in Junkins and Kim [8] it may be shown that asymptotic stability can be concluded since

$$\tilde{L}'' = 0 \quad \text{for all } \mathbf{X} \in Z$$

and

$$\tilde{L}''' < 0 \quad \text{for all } \mathbf{X} \in Z,$$
$$\tilde{L}''' = 0 \quad \text{for all } \mathbf{X} \in \mathbf{X}_{eq},$$

where Z denotes the set of points for which $\tilde{L}'$ vanishes. The constant $\tilde{E}_C$ may be calculated for the first equilibrium point described by $[\theta\ \ \theta'\ \ \phi']^T = [0\ \ 0\ \ \tilde{H}_{Oy}/\tilde{I}]^T$ as

$$\tilde{E}_C = \frac{\tilde{H}_{Oy}^2}{2\tilde{I}}. \tag{B.3}$$

By use of Eqs. (B.1) and (B.3) the Lyapunov function may then be given by

$$\tilde{L} = \frac{(1-\cos X_1)\left(2\tilde{I}\left(\tilde{I} + \sin^2 X_1\right) - \tilde{H}_{Oy}^2(1+\cos X_1)\right) + X_2^2\tilde{I}\left(\tilde{I} - \tilde{d}^2 + \left(1-\tilde{d}^2\right)\sin^2 X_1\right)}{2\tilde{I}\left(\tilde{I} + \sin^2 X_1\right)}. \tag{B.4}$$

By inspection of the terms in the numerator it may be seen that this function is globally positive definite under the conditions

$$\tilde{H}_{Oy}^2 \leqslant \tilde{I}^2 \quad \text{and} \quad \tilde{I} > \tilde{d}^2. \tag{B.5}$$

Using Lyapunov's direct method this first equilibrium point is globally asymptotically stable under these conditions. A similar analysis for the equilibrium points described by $\left[\theta^2 \;\; \theta' \;\; \phi'^2\right]^{\mathrm{T}} = \left[\theta^{*2} \;\; 0 \;\; 1/\cos\theta^*\right]^{\mathrm{T}}$ if $\tilde{H}_{Oy}^2 > \tilde{I}^2$ may also be performed. The constant $\hat{E}_{\mathrm{C}}$ may be calculated as

$$\tilde{E}_{\mathrm{C}} = \tilde{H}_{Oy}^2/2\left(\tilde{I} + \sin^2\theta^*\right) + 1 - \cos\theta^* \tag{B.6}$$

and the Lyapunov function may then be given by

$$\tilde{L} = \frac{\left(\tilde{H}_{Oy}^2\left(\cos^2 X_1 - \cos^2\theta^*\right) - 2\left(\cos X_1 - \cos\theta^*\right)\left(\tilde{I} + \sin^2 X_1\right)\right) + X_2^2\left(\tilde{I} - \tilde{d}^2 + \left(1 - \tilde{d}^2\right)\sin^2 X_1\right)\left(\tilde{I} + \sin^2\theta^*\right)}{2\left(\tilde{I} + \sin^2 X_1\right)\left(\tilde{I} + \sin^2\theta^*\right)}. \tag{B.7}$$

Noting that at equilibrium, the angular momentum is given by

$$\tilde{H}_{Oy}^2 = \left(\tilde{I} + \sin^2\theta^*\right)/\cos\theta^*, \tag{B.8}$$

the terms in the numerator of Eq. (B.7) may be shown to be globally positive definite under the conditions

$$\tilde{H}_{Oy}^2 > \tilde{I}^2 \quad \text{and} \quad \tilde{I} > \tilde{d}^2. \tag{B.9}$$

Using Lyapunov's direct method these equilibrium points are globally asymptotically stable under these conditions. More precisely, it has been shown that all solutions from all initial conditions approach either one of the equilibrium points

$$[\theta \;\; \phi']^{\mathrm{T}} = [\pm\theta^* \;\; 1/\cos\theta^*]^{\mathrm{T}} \quad \text{if } \tilde{H}_{Oy} > \tilde{I} \quad \text{or}$$
$$[\pm\theta^* \;\; -1/\cos\theta^*]^{\mathrm{T}} \quad \text{if } \tilde{H}_{Oy} < -\tilde{I}.$$

It is of note that from the definition of the system inertia, i.e. Eq. (A.6), the condition $\tilde{I} > \tilde{d}^2$ is always satisfied.

References

[1] F.C. Moon, Chaotic and Fractal Dynamics, Wiley, New York, 1992.
[2] P.J. Holmes, J.E. Marsden, Indiana Univ. Math. J. 32 (2) (1983) 273–309.
[3] J. Koiller, J. Math. Phys. 25 (5) (1984) 1599–1604.
[4] P.A. Meehan, Ph.D. Thesis, University of Queensland, 1998.
[5] P.A. Meehan, S.F. Asokanthan, Chaos Soliton Fractal 13 (2002) 1857–1869.
[6] P.I. Corke, G.J. Winstanley, J.M. Roberts, IEEE International Conference on Robotics and Automation, Albuquerque, New Mexico, 1997, pp. 1657–1662.
[7] A.J. Miller, G.L. Gray, A.P. Mazzoleni, J. Guidance, Control Dyn. 24 (3) (2001) 605–615.
[8] J.L. Junkins, Y. Kim, Introduction to Dynamics and Control of Flexible Structures, AIAA, Washington DC, 1993, pp. 90–93.